


Article

Explicit Multipole Formula for the Local Thermal Resistance in an Energy Pile—The Line-Source Approximation

Johan Claesson ¹ and Saqib Javed ^{2,*} ¹ Building Physics, Lund University, 221 00 Lund, Sweden; johan.claesson@byggtek.lth.se² Building Services, Lund University, 221 00 Lund, Sweden

* Correspondence: saqib.javed@hvac.lth.se; Tel.: +46-46-222-1745

Received: 22 September 2020; Accepted: 15 October 2020; Published: 19 October 2020



Abstract: This paper presents a closed-form quite handy formula for the local thermal resistance R_b between the temperature of the bulk heat-carrier fluid in the pipes, equally spaced on a concentric circle inside a circular energy pile, and the mean temperature at the periphery of the pile. The so-called multipole method is used to calculate the temperature field. An important improvement of the multipole method is presented, where Cauchy's mean value theorem of analytical functions is used. The formula for thermal resistance R_{b0} for the zero-order approximation ($J = 0$), where only line heat sources at the pipes are used, is presented. The errors using zeroth-order approximation ($J = 0$) are shown to be quite small by comparisons with eight-order approximation ($J = 8$) with its accuracy of more than eight digits. The relative error for the local thermal resistance R_{b0} for the zero-order approximation ($J = 0$) lies below 5% for a wide range of input parameter values. These ranges are judged to cover most practical cases of application. The smallest local thermal resistance R_{bmin} is, with some exceptions, obtained when the pipes lie directly in contact with the pile periphery. A neat formula for this minimum is presented.

Keywords: energy piles; thermal piles; pile foundations; local thermal resistance; minimum thermal resistance; multipole method; ground source heat pump (GSHP)

1. Introduction

Ground-source heat pump (GSHP) systems are among the most energy-efficient and environmentally clean heating and cooling technologies available today [1]. Due to their higher efficiency, they offer substantial potential for energy savings and carbon emissions reduction in buildings [2]. The most common application of GSHP systems is with vertical borehole heat exchangers [3]. Boreholes are routinely drilled to 100- to 400-m depths and require a specific drilling area as well as specialized drilling equipment. The high capital cost of installing borehole heat exchangers is one of the underlying reasons that hamper the widespread deployment of GSHP systems in many places around the world. For new constructions, an alternative to using borehole heat exchangers is to use piled foundations with embedded heat exchange elements as ground heat exchangers. The thermally active foundation piles, commonly referred to as energy or thermal piles, are dual-function structural elements that transmit mechanical loads through unstable soil layers to lower ground levels with high bearing capacity as well as exchange heat with the surrounding ground to provide heating and cooling to the building. They do not require the capital cost and land requirements of borehole heat exchangers and have the potential to lower the environmental footprint of GSHP systems by using fewer materials with low embodied energy.

Energy piles are constructed in many different configurations, as shown in Figure 1, and have typical diameters varying between 0.1 m and up to 3.0 m and lengths ranging from 10 to 60 m [4].

The number and arrangement of heat transfer pipes in the pile depend on the size and construction method of the energy piles. Driven piles of steel or concrete usually have one to two U-pipes arranged in a series or parallel configuration. The heat transfer pipes are placed towards the center of the pile in the hollow driven piles and are positioned around the reinforcement bars in the solid driven piles. Continuous flight auger (CFA) piles have one to three U-pipes installed in the center of the pile. Bored piles have one to several U-pipes mounted on the reinforcement frame close to the boundary of the pile. The differences in construction methods and geometrical arrangements lead to different thermal characteristics of energy piles.

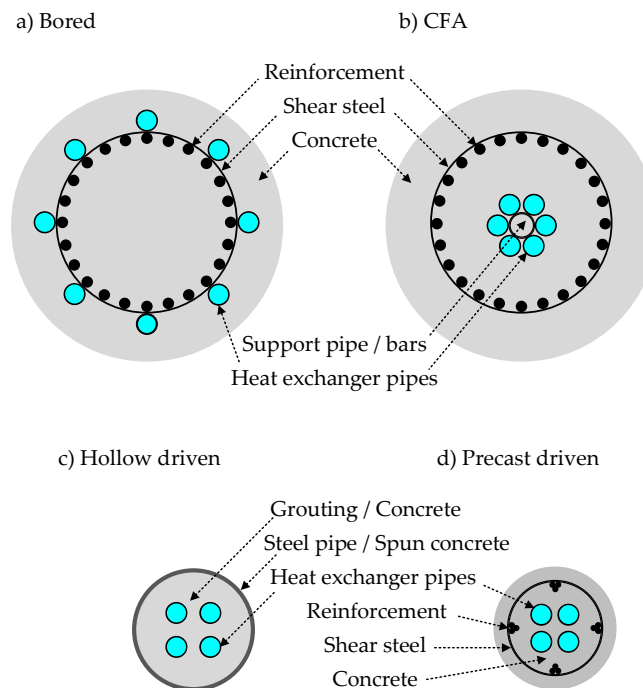


Figure 1. Common types of energy piles.

The current design and analysis methods of energy piles are primarily based on the methods developed for borehole heat exchangers [5]. This is done under the assumption that the thermal characteristics of energy piles and borehole heat exchangers are similar, which is not entirely accurate but simplifies the analysis. Energy piles usually have a greater number of heat transfer pipes and a far smaller aspect (length to diameter) ratio, which differentiates their thermal response from borehole heat exchangers. A key characteristic in this regard is the thermal resistance, which characterizes the heat transfer inside the ground heat exchangers. The thermal resistance R_b of a ground heat exchanger is the ratio of the temperature difference between the circulating fluid in the heat transfer pipes and the surrounding ground to the heat flux per unit length of the ground heat exchanger. The larger number of pipes and their many possible arrangements in energy piles complicate the heat transfer and make the calculation of thermal resistance calculation more complex than for borehole heat exchangers.

There are two main approaches for calculating the thermal resistance of energy piles. In the first approach, thermal resistance is estimated using in situ thermal response testing of energy piles [6,7]. This approach is not generally useful for design purposes as it can only estimate thermal resistance of an existing energy pile. In the second approach, thermal resistance is computed using mathematical models based on conductive heat transfer. Several mathematical models have been proposed and used in this regard. Readers are referred to studies [8–10] for a detailed survey and comparison of these models. Some of the commonly used models for calculating the thermal resistance of energy piles include those of Loveridge and Powrie [11], Paul [12], Sharqawy et al. [13], Bauer et al. [14],

and Diao et al. [15]. A great majority of these models only work well under certain conditions and perform poorly under others [10]. Moreover, among the existing methods, only the Loveridge and Powrie model can calculate the thermal resistance of energy piles with more than two U-pipes. In the absence of suitable analytical methods, the common practice has been to use a conservative estimate of thermal resistance when sizing energy piles with three or more U-pipes.

One of the most robust and accurate methods for calculating the thermal resistance of ground heat exchangers is the multipole method. It is a mathematically rigorous and thoroughly validated analytical method used for calculating the thermal resistances of any number of arbitrarily placed pipes in a composite region. The model, originally developed in the 1980s by Bennet, Claesson, and Hellström [16], uses a combination of line heat sources and so-called multipoles to yield an exact solution of the steady-state temperature field and thermal resistances for arbitrarily placed pipes in a circular region surrounded by an infinite region. The accuracy of the model increases with the number of multipoles used for the calculation. The 10th-order multipole provides a greater than 8-decimal digit accuracy. The original model with 10th-order multipole was provided as a FORTRAN code of approximately 600 lines. It has since been incorporated into several building energy simulation software and ground heat exchanger design programs for calculating the thermal resistance of borehole heat exchangers with single and double U-pipes [17,18]. A principal modification to the model was made in 2011 by Claesson and Hellström [19], who simplified the algorithm by putting a condition on the mean temperature around the periphery of the ground heat exchanger instead of prescribing a constant temperature condition at a suitable radial distance outside the ground heat exchanger in the original model. The modified multipole model is available as a Mathcad program.

The multipole method has a highly sophisticated mathematical formulation and a rather complex algorithm. Its implementation in design and simulation programs is intricate and requires considerable programming expertise and effort. This has led to the development of closed-form multipole formulas that, under certain conditions, can be as accurate as the original multipole method in calculating the thermal resistance of ground heat exchangers. So far, exact multipole formulas have only been developed for single and double U-pipe configurations. Claesson and Javed [20] presented zeroth-, first-, second-, and third-order multipole formulas for single U-pipe ground heat exchangers with symmetrically positioned pipes. Later, the authors also presented zeroth- and first-order multipole formulas for double U-pipe ground heat exchangers with symmetrically positioned pipes [21]. The accuracy of the presented formulas depends upon the order of their multipoles. The zeroth-order multipole formulas only account for line sources and do not consider any multipoles. Javed and Spitler [10] noted that for a single U-pipe borehole heat exchanger the accuracy of the zeroth-order multipole formula varies from case to case. In some cases, the accuracy of the zeroth-order formula is quite good; in other cases, it is not as good. However, the first- and second-order multipole formulas provide an accuracy of better than 3% and 1%, respectively, compared to the original multipole method under all practical conditions [20]. Similar trends have also been observed for double U-pipe ground heat exchangers by Claesson and Javed [21]. The multipole formulas for single and double U-pipe ground heat exchangers are also applicable to energy piles with a corresponding number of U-pipes.

In this paper, an important improvement of the multipole method is presented. Cauchy's so-called mean-value theorem for analytical functions is used to determine the value of certain complex-valued integrals around the pipe periphery (see Section 3). The objective of this paper is to derive a closed-form zeroth-order multipole formula for any number of *evenly* distributed pipes in a ground heat exchanger. The derived formula is applicable for energy piles with multiple U-pipes equally spaced on a circle. The accuracy of the presented formula is established by a detailed parametric study that brackets all or almost all real-world energy piles with a circular cross-section.

2. Energy Pile with Pipes Equally Spaced on a Circle

Figure 2 shows the considered type of energy pile. The N ($=8$) vertical heat exchanger pipes are equally spaced on the circle $r = r_c$. Typical values for N may be in the range from 2 to 12. The left-hand

figure shows a horizontal cross-section of the energy pile and the surrounding ground, and the right-hand figure shows in greater detail the pipe with the center at $(r_c, 0)$ on the positive x -axis.

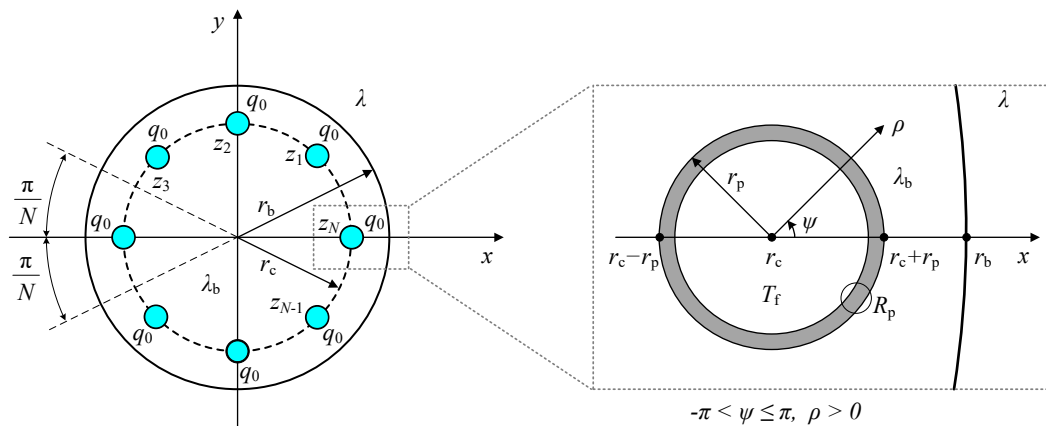


Figure 2. Energy pile with $N (=8)$ heat exchanger pipes equally spaced on the circle $r = r_c$.

The radius of the energy pile is r_b . The index b for borehole is kept from other multiple papers. The thermal conductivity in the ground outside the energy pile, $r > r_b$, is λ (W/(m·K)), and it is λ_b inside the circular energy pile region outside the pipes. The outer radius of the pipes is r_p , and R_p denotes the thermal resistance from bulk fluid in the pipes to the outer pipe wall (per meter pipe, (K·m)/W). The pipe resistance R_p is the sum of the thermal resistances of the pipe wall (an annulus) and the fluid boundary layer.

The heat injection from each pipe to the ground is q_0 (W/m). The value of q_0 is negative for heat extraction from the ground. The required fluid temperature T_f for the heat carrier fluid to achieve the prescribed heat flux q_0 is to be calculated.

The (steady-state) thermal problem requires that an outer ground temperature is prescribed. As will be discussed in Section 6, it is sufficient to prescribe the average temperature T_{bav} around the periphery $r = r_b$ of the energy pile. This way is close to the thermal problem that was first presented in [19].

The thermal problem has a high degree of symmetry. The temperature field in the wedge indicated in the left-hand Figure 2 around the x -axis with the opening angle $\varphi = 2\pi/N$ is repeated around each of the N pipes. The temperature field is symmetric in y , so the upper and lower halves of the wedge mirror each other.

The primary input data are:

$$N, q_0, \lambda_b, \lambda, r_p, r_c, r_b, R_p, T_{bav}. \tag{1}$$

The thermal resistance R_p ((K·m)/W) may be represented by a nondimensional parameter β , and the ratio between the two conductivities by the parameter σ :

$$\beta = 2 \pi \lambda_b R_p, \beta \geq 0, \sigma = \frac{\lambda_b - \lambda}{\lambda_b + \lambda}, -1 < \sigma < 1. \tag{2}$$

The positions of the N pipes on the circle $r = r_c$ become using the complex exponential z_e :

$$z_n = r_c \cdot z_e^n, z_e = e^{\frac{2\pi i}{N}} = \cos(2\pi / N) + i \cdot \sin(2\pi / N), n = 1, 2, \dots, N; \tag{3}$$

$$z_1 = r_c \cdot z_e^1, z_2 = r_c \cdot z_e^2, \dots, z_N = r_c \cdot z_e^N = r_c; |z_e| = 1, \arg(z_e) = \frac{2\pi}{N}.$$

The positions of consecutive pipes are obtained by the complex rotation z_e or increase of the polar angle by $2\pi/N$. The last pipe N lies on the positive x -axis at $z = r_c$.

The circles around the pipes and the pile must not intersect. This gives the following restrictions on r_p , r_c , and r_b for any N :

$$N \geq 2: \frac{r_p}{\sin(\pi/N)} \leq r_c \leq r_b - r_p; \quad N = 1: 0 \leq r_c \leq r_b - r_p, \quad N \leq \frac{\pi}{\arcsin(r_p/(r_b - r_p))}. \quad (4)$$

The lower limit is the case when the pipes are squeezed in the center so that consecutive pipes touch each other. In the upper limit, the pipes touch the wall of the energy pile. The left-hand inequalities give an upper limit for N depending on $r_p/(r_b - r_p)$ as indicated to the right. The pipes may be the two shanks of U-pipes and then N is an even number. However, all formulas in the paper are valid for any N including $N = 1$.

The thermal resistance R_b ((K·m)/W) between the heat carrier fluid in the pipes and the periphery of the energy pile with the *average* temperature T_{bav} is defined by the relation:

$$N q_p \cdot R_b = T_f - T_{bav}, \quad R_b = \frac{1}{K_b} \Rightarrow N q_p = K_b \cdot (T_f - T_{bav}). \quad (5)$$

The inverse of the thermal resistance is the corresponding thermal conductance K_b (W/(K·m)) of the energy pile.

3. The Multipole Method Applied to the Energy Pile

This section presents the application of the multipole method to an energy pile with multiple U-pipes equally spaced on a circle.

3.1. Temperature Field from the N Line Heat Sources

Complex notations and Cartesian and polar coordinates are used:

$$z = x + i \cdot y = r \cdot e^{i\varphi} = r \cdot \cos(\varphi) + i \cdot r \cdot \sin(\varphi), \quad |z| = r = \sqrt{x^2 + y^2}. \quad (6)$$

The complex-valued logarithm of any complex function $f(z)$ is defined by:

$$\ln(f(z)) = \ln(|f(z)|) + i \cdot \arg(f(z)), \quad -\pi < \arg(f(z)) \leq \pi. \quad (7)$$

Explicit expressions for the temperature field are derived in Appendices A.1–A.3. The temperature field has the following form:

$$T(x, y) = T_c(z) = T_{bav} + \frac{q_0}{2\pi\lambda_b} \cdot \operatorname{Re}[W_c(z, r_c)], \quad z = x + i \cdot y \quad (8)$$

where $W_c(z, r_c)$ is obtained from the sum of the N complex-valued line sources in Figure 2, left. The following compact expressions are derived in detail in Appendices A.1–A.3, Equation (A12):

$$W_c(z, r_c) = \begin{cases} \ln\left(\frac{r_b^N}{z^N - r_c^N}\right) + \sigma \cdot \ln\left(\frac{r_b^{2N}}{r_b^{2N} - z^N \cdot r_c^N}\right) & |z| \leq r_b \\ \frac{\lambda_b}{\lambda} \cdot \left[N \cdot \ln\left(\frac{r_b}{z}\right) + \frac{2\lambda}{\lambda_b + \lambda} \cdot \ln\left(\frac{z^N}{z^N - r_c^N}\right) \right] & |z| \geq r_b. \end{cases} \quad (9)$$

The temperature field involves the absolute value of two polynomials in z :

$$P_c(z) = |z^N - r_c^N|, \quad P_\sigma(z) = |r_b^{2N} - z^N \cdot r_c^N|. \quad (10)$$

The formulas for the temperature in the pile and ground regions become:

$$T(x, y) = T_{\text{bav}} + \frac{q_0}{2 \pi \lambda_b} \cdot \left[\ln \left(\frac{r_b^N}{P_c(z)} \right) + \sigma \cdot \ln \left(\frac{r_b^{2N}}{P_\sigma(z)} \right) \right], \quad |z| \leq r_b \quad (11)$$

$$T(x, y) = T_{\text{bav}} + \frac{q_0}{2 \pi \lambda} \cdot \left[N \cdot \ln \left(\frac{r_b}{|z|} \right) + \frac{2 \lambda}{\lambda_b + \lambda} \cdot \ln \left(\frac{|z|^N}{P_c(z)} \right) \right], \quad |z| \geq r_b. \quad (12)$$

This is the line-source solution without using multipoles. The above temperature field satisfies the following conditions:

- Laplace equation in the pile and ground regions,
- The heat flux of q_0 (W/m) from each pipe,
- The internal boundary conditions of continuous temperature at the pile periphery,
- The internal boundary conditions of continuous radial heat flux at the pile periphery (the thermal conductivity is λ_b in the pile region and λ in the outside ground),
- The average temperature of T_{bav} at the pile periphery.

The temperature field in polar coordinates becomes from (11) and (12):

$$T_c(r, e^{i\varphi}) = T_{\text{pol}}(r, \varphi) = T_{\text{bav}} + \begin{cases} \frac{q_0}{2 \pi \lambda_b} \cdot \left[\ln \left(\frac{r_b^N}{P_c(r e^{i\varphi})} \right) + \sigma \cdot \ln \left(\frac{r_b^{2N}}{P_\sigma(r e^{i\varphi})} \right) \right] & r \leq r_b \\ \frac{N \cdot q_0}{2 \pi \lambda} \cdot \ln \left(\frac{r_b}{r} \right) + \frac{q_0}{\pi (\lambda_b + \lambda)} \cdot \ln \left(\frac{r^N}{P_c(r e^{i\varphi})} \right) & r \geq r_b. \end{cases} \quad (13)$$

The two denominators in the logarithms become:

$$\begin{aligned} P_c(r e^{i\varphi}) &= |r^N e^{iN\varphi} - r_c^N| = \sqrt{r^{2N} - 2 r^N r_c^N \cos(N \varphi) + r_c^{2N}}, \\ P_\sigma(r e^{i\varphi}) &= |r_b^{2N} - r^N r_c^N e^{iN\varphi}| = \sqrt{r_b^{4N} - 2 r_b^{2N} r^N r_c^N \cos(N \cdot \varphi) + r^{2N} r_c^{2N}}. \end{aligned} \quad (14)$$

The temperature around the wall of the energy pile becomes:

$$T_{\text{pol}}(r_b, \varphi) = T_{\text{bav}} + \frac{q_0}{\pi (\lambda_b + \lambda)} \cdot \ln \left(\frac{r_b^N}{P_{\text{cb}}(\varphi)} \right), \quad P_{\text{cb}}(\varphi) = \sqrt{r_b^{2N} - 2 r_b^N r_c^N \cos(N \varphi) + r_c^{2N}}. \quad (15)$$

$$P_{\text{cb}}(0) = r_b^N - r_c^N, \quad P_{\text{cb}}(0.5 \pi / N) = \sqrt{r_b^{2N} + r_c^{2N}}, \quad P_{\text{cb}}(\pi / N) = r_b^N + r_c^N. \quad (16)$$

The wall temperature varies around the average T_{bav} roughly following $\cos(N \cdot \varphi)$.

3.2. Boundary Condition at the Pipes

The boundary condition at the periphery of any pipe remains to be fulfilled. It is sufficient to consider pipe N at $z_N = r_c$ due to the rotational symmetry, where the temperature field is repeated for every increase of the polar angle φ by $2\pi/N$. See Figure 2 and the discussion at Equation (A13).

Let ρ be the local *radial distance* from the center of pipe N and ψ the *local polar angle* from this center $z = r_c$ as indicated in Figure 2, right:

$$z = r_c + \rho \cdot e^{i\psi}, \quad 0 < \rho \leq r_b - r_c, \quad -\pi < \psi \leq \pi. \quad (17)$$

The circular region around pipe N inside the energy pile area extends at least to the pipe radius r_p . Let h_p (W/(m²·K)) denote the heat transfer coefficient (per unit pipe area) between the heat carrier

fluid in the pipes and the outer side of the pipe wall. The pipe thermal conductance K_p (W/(m·K)) is obtained by multiplication by the length of the circumference:

$$K_p = 2 \pi r_p \cdot h_p, \quad R_p = \frac{1}{2 \pi r_p \cdot h_p}, \quad \frac{\lambda_b}{h_p} = \lambda_b \cdot 2 \pi r_p \cdot R_p = \beta \cdot r_p. \quad (18)$$

In the right-hand formula, (2), left, is used. The boundary condition involves a heat balance between the radial heat flux at the outside pipe wall and, the difference between the bulk fluid temperature T_f and the temperature outside the pipe multiplied by the heat transfer coefficient h_p . The temperature outside the pipe and the heat flux vary around the pipe with the local polar angle ψ :

$$h_p \cdot [T_f - T_c(r_c + r_p \cdot e^{i\psi})] = q_{pN}(\psi) = (-\lambda_b) \cdot \frac{\partial}{\partial \rho} [T_c(r_c + \rho \cdot e^{i\psi})] \Big|_{\rho=r_p}, \quad -\pi < \psi \leq \pi. \quad (19)$$

It should be noted that the above two heat fluxes have the dimension of W/m².

The above *exact* boundary condition at each point of the periphery may be written in the following way:

$$T_{BC}(\psi) = T_c(r_c + r_p \cdot e^{i\psi}) + \frac{q_{pN}(\psi)}{h_p} = T_f, \quad -\pi < \psi \leq \pi. \quad (20)$$

The sum of the temperature outside the pipe and the radial heat flux over the pipe divided by h_p shall be equal to (a constant) T_f for all ψ . The subscript BC is used to denote this left-hand boundary-condition function of ψ . In a more precise solution, the boundary condition may be fulfilled with increasing accuracy by adding multipole components to the temperature field with suitably adjusted strength factors. This is, however, left to a sequel paper. Here, only line heat sources are used, which means that the boundary condition is fulfilled approximately as a *mean heat balance* for the considered pipe.

The integral of $q_{pN}(\psi)$ around the pipe is equal to the heat flux q_0 . Integration of (20) gives:

$$\int_{-\pi}^{\pi} q_{pN}(\psi) \cdot r_p \, d\psi = q_0, \quad \int_{-\pi}^{\pi} T_c(r_c + r_p \cdot e^{i\psi}) \cdot r_p \, d\psi + \frac{1}{h_p} \cdot q_0 = 2 \pi r_p \cdot T_f. \quad (21)$$

Using (18), center, the following relation between the fluid temperature T_{f0} and the mean temperature outside the pipe is obtained in the present approximation without multipoles ($J = 0$):

$$\frac{1}{2 \pi} \cdot \int_{-\pi}^{\pi} T_c(r_c + r_p \cdot e^{i\psi}) \, d\psi + R_p \cdot q_0 = T_{f0}. \quad (22)$$

The subscript 0 is added for the fluid temperature to underline that it is the value for $J = 0$. The remaining task is now to calculate this mean temperature around the pipe from the temperature field (8) and (9), upper line.

3.3. Mean Temperature at the Outer Periphery of the Pipes

The temperature $T_c(z)$ consists of the line source at $z = r_c$ and a remaining part that is an analytic function of z near $z = r_c$. The direct contributions from the N pipes in (9), upper left, is rewritten in the following way:

$$\ln\left(\frac{r_b^N}{z^N - r_c^N}\right) = \ln\left(\frac{r_b}{z - r_c}\right) + \ln\left(\frac{r_b^N}{z^N - r_c^N} \cdot \frac{z - r_c}{r_b}\right) = \ln\left(\frac{r_b}{z - r_c}\right) + \ln\left(\frac{r_b^{N-1}}{S(z, r_c)}\right), \quad (23)$$

$$\frac{z^N - r_c^N}{z - r_c} = S(z, r_c) = \sum_{n=1}^N z^{N-n} \cdot r_c^{n-1}, \quad S(r_c, r_c) = N \cdot r_c^{N-1}.$$

The full solution $W_c(z, r_c)$ consists of the line source with its singularity at $z = r_c$ and an analytic part $W_a(z, r_c)$:

$$W_c(z, r_c) = \ln\left(\frac{r_b}{z - r_c}\right) + W_a(z, r_c), \quad W_a(z, r_c) = \ln\left(\frac{r_b^{N-1}}{S(z, r_c)}\right) + \sigma \cdot \ln\left(\frac{r_b^{2N}}{r_b^{2N} - z^N \cdot r_c^N}\right). \quad (24)$$

The integral of the line source becomes:

$$\frac{1}{2\pi} \cdot \int_{-\pi}^{\pi} \operatorname{Re}\left[\ln\left(\frac{r_b}{r_c + r_p \cdot e^{i\psi} - r_c}\right)\right] d\psi = \frac{1}{2\pi} \cdot \int_{-\pi}^{\pi} \operatorname{Re}\left[\ln\left(\frac{r_b}{r_p \cdot e^{i\psi}}\right)\right] d\psi = \ln\left(\frac{r_b}{r_p}\right). \quad (25)$$

There is a nice *mean-value theorem* for analytic functions by Cauchy, which is directly applicable to the integral of $W_a(z, r_c)$ around the pipe at $z = r_c$. Let $f(z)$ be a function that is analytic on and inside a circle with the radius r_p around a point z_0 in the complex z -plane. Then, the mean value of the function on the circle is equal to the value of $f(z)$ at the center of the circle:

$$\frac{1}{2\pi} \cdot \int_{-\pi}^{\pi} f(z_0 + r_p \cdot e^{i\psi}) d\psi = f(z_0), \quad f(z) \text{ analytic in } |z - z_0| \leq r_p. \quad (26)$$

This formula may be found in any standard book on analytical functions, for example [22]. An important idea in the improved new approach to the multipole technique presented here is to use this mean-value theorem for the analytic function $W_a(z, r_c)$:

$$\frac{1}{2\pi} \cdot \int_{-\pi}^{\pi} W_a(r_c + r_p \cdot e^{i\psi}, r_c) d\psi = W_a(r_c, r_c). \quad (27)$$

The integral of T_c around the pipe in (22) gets a logarithmic contribution (25) from the line source and another one (27) from the analytical part:

$$\frac{1}{2\pi} \cdot \int_{-\pi}^{\pi} T_c(r_c + r_p \cdot e^{i\psi}) d\psi = T_{\text{bav}} + \frac{q_0}{2\pi \lambda_b} \cdot \left[\ln\left(\frac{r_b}{r_p}\right) + \operatorname{Re}[W_a(r_c, r_c)] \right]. \quad (28)$$

The value of $W_a(z, r_c)$ for $z = r_c$ is from (23) and (24):

$$W_a(r_c, r_c) = \ln\left(\frac{r_b^{N-1}}{N \cdot r_c^{N-1}}\right) + \sigma \cdot \ln\left(\frac{r_b^{2N}}{r_b^{2N} - r_c^{2N}}\right). \quad (29)$$

The fluid temperature now becomes from (22), (27), and (29):

$$T_{f0} = T_{\text{bav}} + R_p \cdot q_0 + \frac{q_0}{2\pi \lambda_b} \cdot \left[\ln\left(\frac{r_b}{r_p}\right) + \ln\left(\frac{r_b^{N-1}}{N \cdot r_c^{N-1}}\right) + \sigma \cdot \ln\left(\frac{r_b^{2N}}{r_b^{2N} - r_c^{2N}}\right) \right]. \quad (30)$$

4. Thermal Resistance of the Energy Pile

The main goal of this paper is to derive a formula for the (local, steady-state) thermal resistance between the heat carrier fluid in the pipes and the periphery of the energy pile with its prescribed average temperature T_{bav} . This resistance becomes from (5) and (30):

$$R_{b0} = \frac{T_{f0} - T_{\text{bav}}}{N q_0} = \frac{R_p}{N} + \frac{1}{N \cdot 2\pi \lambda_b} \cdot \left[\ln\left(\frac{r_b}{N \cdot r_p \cdot r_c^{N-1}}\right) + \sigma \cdot \ln\left(\frac{r_b^{2N}}{r_b^{2N} - r_c^{2N}}\right) \right]. \quad (31)$$

The formula is based on the line-source approximation for the temperature field. An important task is then to determine the accuracy of the formula for various input parameter values; see Section 8.

4.1. The Thermal Resistance R_{b0} as a Function of r_c

The thermal resistance R_{b0} of the energy pile depends on the input parameters (1) and in particular on the radial distance r_c from the center $z = 0$ to the pipes. Equation (31) may be written as:

$$R_b = \frac{R_p}{N} + \frac{1}{N \cdot 2 \pi \lambda_b} \cdot \left[\ln\left(\frac{r_b}{N \cdot r_p}\right) + R'(r_c) \right]. \quad (32)$$

The dependence on r_c is expressed by the function $R'(r_c)$:

$$R'(r_c) = (N - 1) \cdot \ln\left(\frac{r_b}{r_c}\right) + \sigma \cdot \ln\left(\frac{r_b^{2N}}{r_b^{2N} - r_c^{2N}}\right), \quad r_c \leq r_b - r_p. \quad (33)$$

The range of allowed values for r_c is limited by the restrictions that the circles of pipes and energy pile must not intersect each other, (4).

An interesting question is now what is the best choice for r_c ? The thermal resistance shall be as small as possible. The resistance should normally decrease as the distance to the pile periphery decreases. The derivative of $R'(r_c)$ is readily obtained from (33):

$$\frac{dR'}{dr_c} = -\frac{N-1}{r_c} + \sigma \cdot \frac{2N \cdot r_c^{2N-1}}{r_b^{2N} - r_c^{2N}} = -\frac{2N \cdot r_c^{2N-1}}{r_b^{2N} - r_c^{2N}} \cdot \left[\frac{N-1}{2N} \cdot \frac{r_b^{2N} - r_c^{2N}}{r_c^{2N}} - \sigma \right]. \quad (34)$$

The derivative is negative for all r_c if σ is negative, i.e., $\lambda_b \leq \lambda$. Then, the minimum occurs at the right end $r_c = r_b - r_p$. The derivative becomes positive if the right-hand expression within the square brackets is negative. This *may* happen for larger ratios of λ_b/λ and r_c close to $r_b - r_p$, but for N greater than, say 5, the minimum lies very close to the right-hand limit, and this limit can be used quite safely in the present applications to determine the minimum of R_{b0} : $R_{bmin} = R_{b0}|_{r_c=r_b-r_p}$.

For λ_b larger than λ , it may be better to distance the pipes slightly from the energy pile periphery to avoid too much heat flow in the ground region with its lower conductivity. The effect on the minimum is, however, negligible in the present applications. For the cases $N = 1, 2, 3, 4$, the effect is somewhat greater and worth considering.

4.2. Minimum Thermal Resistance for $r_c = r_b - r_p$

The minimum value for the thermal resistance of the energy pile occurs exactly or with good accuracy when the pipes touch the periphery of the energy pile. The formula for the minimum is obtained from (31):

$$R_{bmin} = \frac{R_p}{N} + \frac{1}{N \cdot 2 \pi \lambda_b} \cdot \left[\ln\left(\frac{r_b^N}{N \cdot r_p (r_b - r_p)^{N-1}}\right) + \sigma \cdot \ln\left(\frac{r_b^{2N}}{r_b^{2N} - (r_b - r_p)^{2N}}\right) \right]. \quad (35)$$

The minimum resistance depends on the ratio r_p/r_b in the following way:

$$R_{bmin} = \frac{R_p}{N} + \frac{1}{2 \pi \lambda_b N} \cdot R''(r'_p), \quad r'_p = \frac{r_p}{r_b}, \quad r_c = r_b - r_p, \\ R''(r'_p) = \ln\left(\frac{1}{N r'_p}\right) + (N - 1) \cdot \ln\left(\frac{1}{1 - r'_p}\right) + \sigma \cdot \ln\left(\frac{1}{1 - (1 - r'_p)^{2N}}\right). \quad (36)$$

The ratio r_p/r_b is rather small. The following approximation (derived from suitable Taylor expansions of the logarithms) shows the behavior for small ratios:

$$R''(r'_p) \approx \ln\left(\frac{1}{N r'_p}\right) + (N-1) \cdot \left(r'_p + 0.5 \cdot (r'_p)^2\right) + \sigma \cdot \left[\ln\left(\frac{1}{2 N r'_p}\right) + (N-0.5) \cdot \left(r'_p - \frac{2N-5}{12} \cdot (r'_p)^2\right)\right]. \quad (37)$$

The two quadratic terms in r'_p may be neglected for say $r'_p \leq 0.1$. The minimum resistance of the energy pile when the pipes touch the pile wall, $r_c = r_b - r_p$, becomes, with good accuracy:

$$R_{b\text{main}} \approx \frac{R_p}{N} + \frac{1}{N \cdot 2 \pi \lambda_b} \cdot \left\{ (1 + \sigma) \cdot \left[\ln\left(\frac{r_b}{N r_p}\right) + \frac{(N-1) \cdot r_p}{r_b} \right] - \sigma [\ln(2) - 0.5] \cdot \frac{r_p}{r_b} \right\}. \quad (38)$$

5. Formulas and Graphs for the Temperature Field

The temperature field in Cartesian and polar coordinates is given in Section 3.1, Equations (11)–(14). Here, the temperature field is plotted and discussed for a reference case.

5.1. Reference Case

The following data are chosen as the reference case:

$$N = 8, \quad q_0 = 10 \text{ W/m}, \quad \lambda_b = 1.5 \text{ W/(m} \cdot \text{K)}, \quad \lambda = 3 \text{ W/(m} \cdot \text{K)}, \\ 2 \cdot r_b = 0.6 \text{ m}, \quad r_c = r_b - r_p, \quad 2 \cdot r_p = 0.032 \text{ m}, \quad \beta = 0.75, \quad T_{\text{bav}} = 0 \text{ }^\circ\text{C}. \quad (39)$$

The pipe resistance R_p and the conductivity parameter σ become:

$$R_p = \frac{\beta}{2 \pi \lambda_b} = 0.0796 \text{ m} \cdot \text{K/W}, \quad \sigma = \frac{\lambda_b - \lambda}{\lambda_b + \lambda} = -\frac{1}{3}. \quad (40)$$

The average temperature T_{bav} at the pile wall is put to zero in all formulas and graphs below for simplicity. The resistance of the energy pile and the fluid temperature become (31):

$$R_{b0} = 0.024 \text{ m} \cdot \text{K/W}, \quad K_{b0} = 1/R_{b0} = 41.7, \quad T_{f0} = R_{b0} \cdot N q_p = 1.916. \quad (41)$$

5.2. Plots of the Temperature Field

The overall temperature field $T(x, y) = T_{\text{pol}}(r, \varphi)$ for the reference case (39) is presented in Figure 3, left. Six isotherms, $T = 1, 0, -1, -2, -3, -4$, are shown. The black circle $r = r_b$ shows the periphery of the energy pipe. The isotherm $T = 0$ winds around the pile periphery along which the average temperature is zero. The pipes with the fluid temperature $T_{f0} = 1.916$ in heat carrier fluid lie inside the $N = 8$ isothermal circles for $T = 1$. The temperatures at a few particular points become:

$$T(0, 0) = 0.465, \quad T_{\text{pol}}(r_b, 0) = 0.733, \quad T_{\text{pol}}\left(r_b, \frac{\pi}{N}\right) = -0.352, \\ T(r_c + r_p, 0) = 0.733, \quad T(r_c, r_p) = 1.16, \quad T(r_c - r_p, 0) = 1.41. \quad (42)$$

The isotherm $T = -1$ has a wavy form influenced by the position of the pipes. The deviation from a circle decreases outwardly. The isotherm $T = -3$ is very close to a perfect circle.

Figure 3, right, shows a surface plot of the temperature field for the reference case. The pipes are clearly seen as temperature spikes. The very flat region around the center $z = 0$ with values close to $T(0, 0) = 0.465$ is to be noted.

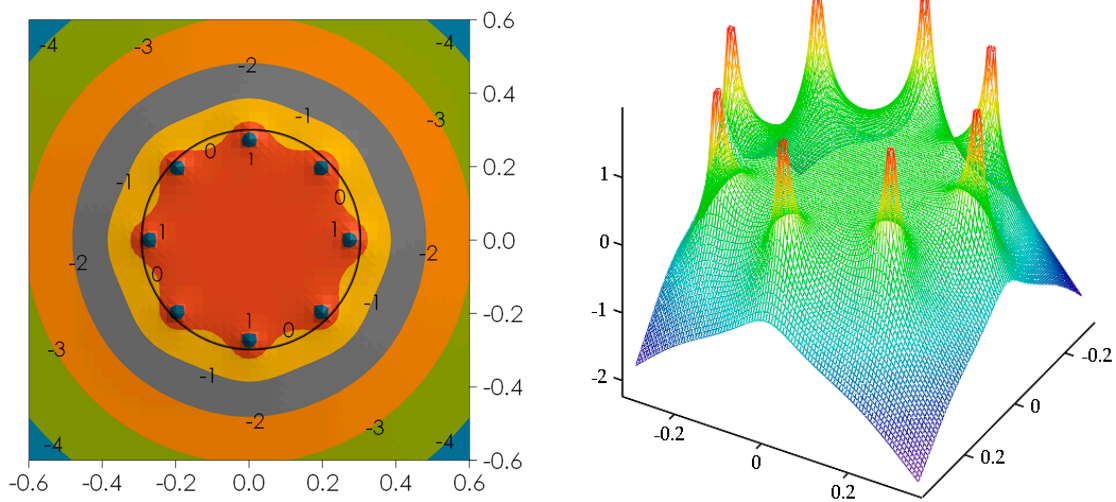


Figure 3. Temperature field (left) and surface plot of the temperature field (right) for the reference case (39).

Figure 4 shows radial profiles $T_{\text{pol}}(r, \varphi)$ from (13) and (14) in the interval $0.2 < r < 0.5$ for $\varphi = 0, \pi/(5N), (3\pi)/(5N),$ and π/N . The red top curve for $\varphi = 0$ tends to infinity at the position $r = r_c$ of the line source. The bottom curve shows the radial profile for the radial line $\varphi = \pi/N$, which lies in the middle between pipe $n = N$ and pipe $n = 1$ in Figure 2. The black dotted line shows the radial average temperature $T_{\text{polav}}(r)$, which is defined below in (46). The four curves converge to the radial average temperature for r greater than 0.4. The difference between the top and bottom curve is 0.091, 0.015, 0.004, and 0.00006 at $r = 0.4, 0.5, 0.6,$ and 1, respectively.

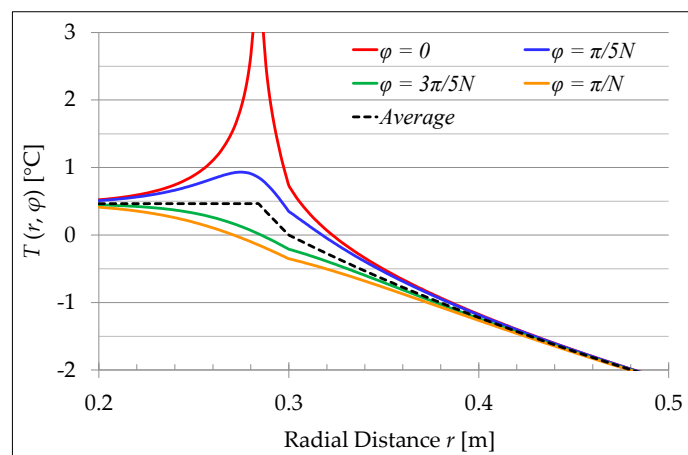


Figure 4. Radial temperature profiles for $\varphi = 0, \pi/(5N), 3\pi/(5N),$ and π/N . The dotted curve shows the average temperature $T_{\text{polav}}(r)$, (46).

The four curves lie very close to the value $T(0, 0) = 0.465$ at the center for $0 < r < 0.2$. The deviation from temperature at $r = 0$ is less than 0.0002 for $r < 0.1$ and less than 0.06 for $r < 0.2$. The temperature field is very flat in the center region of Figure 3 (left) and 3 (right). This means that changes in the thermal conductivity or introduction of a return pipe with the same fluid temperature in the central region $r < 0.2$ will have a negligible, or perhaps marginal, effect on the value of the thermal resistance.

6. Total Radial Heat Flux: Thermal Resistance to Any Radius $r > r_b$

The Laplace equation in polar coordinates for a thermal conductivity that depends on r reads:

$$\frac{1}{r} \cdot \frac{\partial}{\partial r} \left(r \cdot \lambda(r) \frac{\partial T_{\text{pol}}}{\partial r} \right) + \frac{1}{r^2} \cdot \frac{\partial}{\partial \varphi} \left(\lambda(r) \frac{\partial T_{\text{pol}}}{\partial \varphi} \right) = 0, \quad \lambda(r) = \begin{cases} \lambda_b & r < r_b \\ \lambda & r > r_b \end{cases}. \quad (43)$$

The equation is valid everywhere except at the N heat sources on the circle $r = r_c$. Let $T_{\text{polav}}(r)$ denote the average temperature obtained from integration over $-\pi < \varphi < \pi$. Integration of (43) in φ gives:

$$T_{\text{polav}}(r) = \frac{1}{2\pi} \int_{-\pi}^{\pi} T_{\text{pol}}(r, \varphi) d\varphi \Rightarrow \frac{1}{r} \cdot \frac{d}{dr} \left[r \cdot \lambda(r) \frac{dT_{\text{polav}}}{dr} \right] + \frac{1}{r^2} \cdot \left[\lambda(r) \cdot \frac{\partial T_{\text{pol}}}{\partial \varphi} \right]_{\varphi=-\pi}^{\varphi=\pi} = 0. \quad (44)$$

The heat flux in the φ -direction is the same at $\varphi = \pi$ and $\varphi = -\pi$. The right-hand term above vanishes and the average temperature $T_{\text{polav}}(r)$ satisfies the *one-dimensional* radial heat conduction equation except at $r = r_c$, where the total radial heat flux $q_{\text{totrad}}(r)$ increases from zero to $N \cdot q_0$:

$$\frac{d}{dr} \left[r \cdot \lambda(r) \frac{dT_{\text{polav}}}{dr} \right] = 0, \quad r \neq r_c; \quad q_{\text{totrad}}(r) = -2\pi r \cdot \lambda(r) \frac{dT_{\text{polav}}}{dr} = \begin{cases} 0 & r < r_c \\ N q_0 & r > r_c \end{cases}. \quad (45)$$

The temperature $T_{\text{polav}}(r)$ becomes constant for $r < r_c$. It is zero at $r = r_b$ (for $T_{\text{bav}} = 0$) and it varies logarithmically as $\ln(r_b/r)$ for $r > r_c$, inversely proportional to the thermal conductivities λ_b and λ :

$$T_{\text{polav}}(r_b) = 0 \Rightarrow T_{\text{polav}}(r) = \frac{N q_0}{2\pi\lambda} \cdot \ln\left(\frac{r_b}{r}\right), \quad r \geq r_b; \\ T_{\text{polav}}(r) = \frac{N q_0}{2\pi\lambda_b} \cdot \ln\left(\frac{r_b}{r}\right), \quad r_c \leq r \leq r_b, \quad T_{\text{polav}}(r) = \frac{N q_0}{2\pi\lambda_b} \cdot \ln\left(\frac{r_b}{r_c}\right), \quad 0 \leq r \leq r_c. \quad (46)$$

This average temperature is shown by the dotted line in Figure 4. It should be noted that the derivative of the average temperature is discontinuous at $r = r_b$ following $\lambda(r)$, (43) right, while the heat flux is continuous. It should also be noted that $T_{\text{polav}}(0)$ from (46), right, gives the same value $T(0) = 0.465$ as in (42).

The thermal resistance R_b refers to the resistance between the fluid in the pipes and the average temperature at the periphery of the energy pile, (5). The corresponding thermal resistance between the fluid in the pipes and the average temperature at any radius $r_0 > r_b$ is obtained in the following way:

$$r_0 > r_b: T_f - T_{\text{polav}}(r_0) = T_f - T_{\text{polav}}(r_b) + T_{\text{polav}}(r_b) - T_{\text{polav}}(r_0) = N q_0 \cdot R_b - \frac{N q_0}{2\pi\lambda} \cdot \ln\left(\frac{r_b}{r_0}\right). \quad (47)$$

The resistance from fluid to $r = r_0$ becomes equal to the sum of R_b and the thermal resistance of the annular region $r_b < r < r_0$ with its thermal conductivity λ :

$$R_{f \text{ to } r_0} = R_b + \frac{1}{2\pi\lambda} \cdot \ln\left(\frac{r_0}{r_b}\right), \quad r_0 > r_b. \quad (48)$$

This simple thermal network is illustrated in Figure 5.

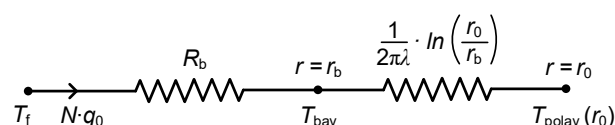


Figure 5. Thermal resistance network between the fluid in the pipes and the average temperature at any radius $r_0 > r_b$.

7. Deviation from the Exact Boundary Condition at the Pipes

The boundary condition at the pipes is discussed in Section 3.2. Equation (20) gives the exact boundary condition at the periphery of the pipes:

$$T_{BC}(\psi) = T_c(r_c + r_p \cdot e^{i\psi}) + \frac{q_{pN}(\psi)}{h_p} = T_f, \quad -\pi < \psi \leq \pi. \tag{49}$$

The temperature at the outside of the pipe as a function of z is given by (8) and (9), top line. The radial heat flux $q_{\rho N}(\psi)$ is defined in (19), right. It is fairly straight-forward to determine this radial derivative with respect to ρ from the formula for the temperature:

$$q_{\rho N}(\psi) = \frac{N q_0}{2 \pi} \cdot \text{Re} \left[\frac{z(\psi)^{N-1} \cdot e^{i\psi}}{z(\psi)^N - r_c^N} - \sigma \cdot \frac{z(\psi)^{N-1} \cdot e^{i\psi} r_c^N}{r_b^{2N} - z(\psi)^N r_c^N} \right], \quad z(\psi) = r_c + r_p \cdot e^{i\psi}. \tag{50}$$

This gives an explicit formula for $T_{BC}(\psi)$.

Figure 6 shows the function (49) for the exact boundary condition around the periphery of the pipes for the reference case (39). The chosen fluid temperature T_{f0} is the average or mean value of the boundary function over ψ as derived above in Section 3.2, Equations (28) and (30). The difference between the two curves represents the deviation from the exact boundary condition. The largest difference 0.092 between $T_{BC}(\psi)$ and the chosen T_{f0} occurs at $\psi = \pm\pi$. The relative error lies below 5%. The temperature at the outside of the pipe and the radial heat flux q_{pN} , (50), divided by the heat transfer coefficient h_p are also shown. These curves vary more than $T_{BC}(\psi)$, but they counteract each other so that the deviation in the boundary condition is much smaller.

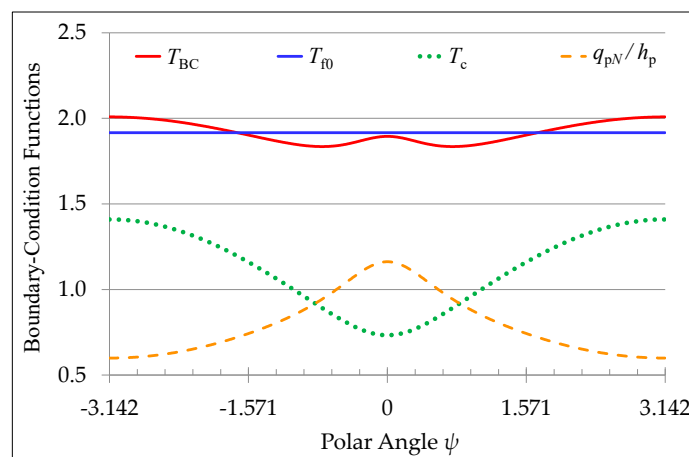


Figure 6. Boundary-condition function $T_{BC}(\psi)$ (49), and its average T_{f0} . The dotted curves show the boundary temperature and the radial heat flux divided by the heat transfer coefficient (50).

8. Comparison with Exact Results from Multipoles Solutions of Order $J = 8$

Higher-order multipole solutions ($J = 1, 2, \dots$) give the thermal resistance with increasing accuracy. The general solution for any order of multipoles J will be reported in a sequel paper. Multipoles up to $J = 8$ are used in the comparisons of accuracy for the thermal resistance of the energy pile.

8.1. Error for $R_b(J)$ as a Function of J

The error for $R_b(J)$ compared to $R_b(8)$ is:

$$\Delta R_b(J) = \frac{R_b(J) - R_b(8)}{R_b(8)} = \frac{T_f(J) - T_f(8)}{T_f(8)}, \quad J = 0, 1, \dots, 7. \tag{51}$$

Figure 7 shows the absolute relative error $|\Delta R_b(J)|$ for $J = 0, 1, \dots, 7$ for the reference case.

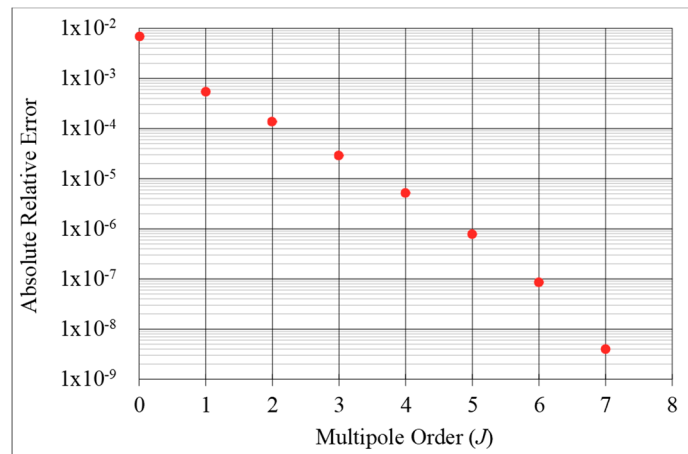


Figure 7. Absolute relative error ΔR_b for $J = 0, 1, 2, \dots, 7$ for the reference case (39).

The relative error for $J = 0$ is 0.0069 or 0.69%. There is a dramatic increase in accuracy with increasing J . This is typical for the multipole method. The multipole method gives the solution and in particular the thermal resistance R_b (8) with 8 digits of accuracy. The error for thermal resistance is always much smaller than the relative deviations for the boundary conditions at the pipes; see Figure 6.

8.2. Relative Error $\Delta R_{b0}(N, r_b, r_c, r_p, \sigma, \beta)$ for a Suitable Set of Parameter Values

The input parameters (1) determine the temperature field and the thermal resistance of the energy pile. The temperature field (11) and (12) is proportional to q_0/λ_b . The non-dimensional relative error $\Delta R_{b0} = \Delta R_b(0)$ with $J = 0$ in (51) will depend on the number of pipes N , two dimensionless parameters, and the three radii:

$$\Delta R_{b0} = \Delta R_{b0}(N, \sigma, \beta, r_p, r_c, r_b); \quad \frac{r_p}{\sin(\pi/N)} \leq r_c \leq r_b - r_p, \quad \beta \geq 0, \quad -1 < \sigma < 1. \quad (52)$$

It may be noted that the relative error is unchanged when the three radii are scaled with the same factor $k > 0$:

$$\Delta R_{b0}(N, \sigma, \beta, r_p, r_c, r_b) = \Delta R_{b0}(N, \sigma, \beta, k \cdot r_p, k \cdot r_c, k \cdot r_b). \quad (53)$$

To investigate the performance of the proposed formula, a parametric study is made, varying the number of pipes N , the pile and ground thermal conductivities, the dimensionless pipe thermal resistance, and the pile geometry. The parameters and levels for the full parametric study, representing $6 \times 5 \times 3 \times 3 \times 4 = 1080$ cases, are summarized in (54):

$$N = 2, 4, 6, 8, 10, 12; \quad 2 \cdot r_b = 0.16, 0.3, 0.6, 1.2, 2.4; \quad r_c = r_{c,\min}, \frac{2r_b}{3}, r_b - r_p; \quad (54)$$

$$2 \cdot r_p = 0.032; \quad \lambda_b / \lambda = 0.5, 1, 2, \quad \text{or } \sigma = -\frac{1}{3}, 0, \frac{1}{3}; \quad \beta = 0.25, 0.5, 1, 2.$$

These first 3 parameters represent 90 different geometries; in all cases, the outer diameter of the U-pipe is 0.032 m. The pile diameters are between 0.16 and 2.4 m. The smallest diameter is smaller than a typical precast driven thermal pile and the largest diameter is closer to what might be found in a large CFA or bored thermal pile. Taken together, the considered diameters bracket almost all energy pile installations. The three r_c radii correspond to close, moderate, and wide pipe spacings. The pipes touch each other and the wall of the energy pile for r_c equal to $r_{c,\min}$ (close spacing), and r_c equal to $r_b - r_p$ (wide spacing), respectively. These cases are typical of CFA and hollow driven piles, respectively. The case r_c equal to $2r_b/3$ (moderate spacing) is representative of a bored energy pile where heat exchanger pipes are mounted on the reinforcement ring. Again, the three spacings virtually

bracket all possible spacings. Similarly, the three levels of sigma bracket the most likely ratios of the borehole and ground thermal conductivities found in practice.

Table 1 shows the relative errors $\Delta R_{b0}(N, r_b, r_c, r_p, \sigma, \beta)$ in percent. The grey cells in the table indicate relative errors of 10% or more. More than 50% of the errors are marked as zero, which means that the error is below 0.5%. For r_b greater than or equal to 0.3 m, the relative error $\Delta R_{b0}(N, r_b, r_c, r_p, \sigma, \beta)$ is less than or equal to 5% for 643 of the 648 cases and less than 10% for all cases. For $r_b = 0.15$ m, the relative error $\Delta R_{b0}(N, r_b, r_c, r_p, \sigma, \beta)$ is less than or equal to 5% for 156 of the 216 cases and less than 10% for all except a few cases. The relative error exceeds 10% only for 8 cases when N is greater than or equal to 8 and β is equal to 0.25 or 0.50 (i.e., for very low R_p and R_b values). These cases are very unlikely in practice and are possible only under the implausible conditions of extremely low thermal conductivity of energy piles and laminar flow in the heat exchanger pipes. Moreover, although the relative error in these cases is large, the absolute error is small and of the order of 0.002 (K·m)/W or less. For r_b equal to 0.08 m, the relative error $\Delta R_{b0}(N, r_b, r_c, r_p, \sigma, \beta)$ is greater than 10% for over one-third of the considered cases. With N equal to 12 and r_p equal to 0.016 m, the $r_{c,min}$ becomes larger than $2r_b/3$, and hence the moderate spacing condition does not hold. The relative error for these cases with r_b equal to 0.08 m is classified as not applicable (n/a) in Table 1. An interesting observation from Table 1 is that the relative error $\Delta R_{b0}(N, r_b, r_c, r_p, \sigma, \beta)$ is positive for β less than 1 and is negative for β larger than 1. This suggests that the zero-order formula overestimates the thermal resistance of energy piles for β less than 1 and underestimates the thermal resistance for β greater than 1. For all cases with β equal to 1, the relative error is fairly close to zero. This information is valuable when setting margins of safety for design.

One parameter that can affect the accuracy of the multipole Formula (39) is the pipe radius. To demonstrate the impact of different pipe radii on the relative errors of the parametric study (54), Tables 2 and 3 present relative errors $\Delta R_{b0}(N, r_b, r_c, r_p, \sigma, \beta)$ for r_b equal to 150 mm and r_p equal to 12.5 mm, and r_b equal to 300 mm and r_p equal to 20 mm, respectively. Comparing the results of Tables 1 and 2 indicates that for energy piles with r_b equal to 0.150 m, the relative errors $\Delta R_{b0}(N, r_b, r_c, r_p, \sigma, \beta)$ become considerably lower for r_p equal to 0.0125 m than for r_p equal to 0.016 m. For r_p equal to 0.0125 m, the relative error exceeds 10% only when N is greater than or equal to 10, and β equal to 0.25. Comparison of the results of Tables 1 and 3 shows that for energy piles with r_b equal to 0.3 m, the relative errors $\Delta R_{b0}(N, r_b, r_c, r_p, \sigma, \beta)$ are marginally higher for r_p equal to 0.02 m than for r_p equal to 0.016 m. Nevertheless, the relative error for r_p equal to 0.02 m exceeds 10% only for the single case of N equal to 12, σ equal to -0.33 , and β equal to 0.25.

Table 1. Relative error ΔR_{b0} ($N, r_b, r_c, r_p, \sigma, \beta$) in percent for $N = 2$ to 12, and $r_c = r_{c,\min}$ (close spacing), $2r_b/3$ (moderate spacing), and $r_b - r_p$ (wide spacing)^a. The pipe radius r_p is 0.016 mm.

r_b (mm)	σ	β	Close						Moderate						Wide					
			2	4	6	8	10	12	2	4	6	8	10	12	2	4	6	8	10	12
80	-0.33	0.25	5	13	17	21	31	65	2	8	17	25	33	n/a	3	12	27	46	65	85
		0.50	3	7	9	12	16	28	1	4	8	12	16	n/a	1	5	11	18	26	32
		1.00	0	0	0	-1	-1	-2	0	0	0	0	-1	n/a	0	0	0	0	-1	-2
		2.00	-3	-8	-10	-13	-16	-21	0	-2	-5	-9	-15	n/a	-1	-2	-5	-9	-14	-21
	0.00	0.25	5	13	17	21	31	64	1	7	16	25	33	n/a	1	8	22	41	61	82
		0.50	3	7	9	12	16	28	0	3	8	12	16	n/a	0	3	9	17	25	32
		1.00	0	0	0	-1	-1	-2	0	0	0	0	-1	n/a	0	0	0	0	-1	-2
		2.00	-3	-8	-10	-13	-16	-21	0	-2	-5	-9	-15	n/a	0	-2	-5	-9	-14	-21
	0.33	0.25	5	13	17	21	31	63	0	7	16	25	33	n/a	0	5	18	37	58	79
		0.50	3	7	9	12	16	27	0	3	8	12	16	n/a	0	2	8	16	24	31
		1.00	0	0	0	-1	-1	-2	0	0	0	0	-1	n/a	0	0	0	0	-1	-2
		2.00	-3	-8	-10	-13	-16	-21	0	-2	-5	-9	-15	n/a	0	-1	-4	-8	-14	-21
150	-0.33	0.25	3	8	9	9	9	10	0	2	4	6	8	9	2	4	9	14	21	29
		0.50	2	5	5	5	5	6	0	1	2	3	4	5	1	2	4	6	9	12
		1.00	0	0	0	0	0	0	0	0	0	0	0	0	0	0	0	0	0	0
		2.00	-2	-6	-7	-7	-8	-8	0	-1	-2	-3	-5	-7	0	-1	-2	-3	-4	-5
	0.00	0.25	3	8	9	9	9	10	0	2	4	6	8	9	0	1	4	9	16	23
		0.50	2	5	5	5	5	6	0	1	2	3	4	5	0	1	2	4	7	10
		1.00	0	0	0	0	0	0	0	0	0	0	0	0	0	0	0	0	0	0
		2.00	-2	-6	-7	-7	-8	-8	0	-1	-2	-3	-5	-7	0	0	-1	-2	-3	-5
	0.33	0.25	3	8	9	9	9	10	0	2	4	6	8	9	0	0	2	6	12	19
		0.50	2	5	5	5	5	6	0	1	2	3	4	5	0	0	1	3	5	9
		1.00	0	0	0	0	0	0	0	0	0	0	0	0	0	0	0	0	0	0
		2.00	-2	-6	-7	-7	-8	-8	0	-1	-2	-3	-5	-7	0	0	-1	-1	-3	-4

Table 1. Cont.

r_b (mm)	σ	β	Close						Moderate						Wide						
			2	4	6	8	10	12	2	4	6	8	10	12	2	4	6	8	10	12	
1200	-0.33	0.25	2	3	3	3	3	3	0	0	0	0	0	0	0	1	1	1	1	2	2
		0.50	1	2	2	2	2	2	0	0	0	0	0	0	0	0	0	0	1	1	1
		1.00	0	0	0	0	0	0	0	0	0	0	0	0	0	0	0	0	0	0	0
		2.00	-1	-3	-3	-3	-3	-3	0	0	0	0	0	0	0	0	0	0	0	0	0
	0.00	0.25	2	3	3	3	3	3	0	0	0	0	0	0	0	0	0	0	0	0	0
		0.50	1	2	2	2	2	2	0	0	0	0	0	0	0	0	0	0	0	0	0
		1.00	0	0	0	0	0	0	0	0	0	0	0	0	0	0	0	0	0	0	0
		2.00	-1	-3	-3	-3	-3	-3	0	0	0	0	0	0	0	0	0	0	0	0	0
	0.33	0.25	2	3	3	3	3	3	0	0	0	0	0	0	0	0	0	0	0	0	0
		0.50	1	2	2	2	2	2	0	0	0	0	0	0	0	0	0	0	0	0	0
		1.00	0	0	0	0	0	0	0	0	0	0	0	0	0	0	0	0	0	0	0
		2.00	-1	-3	-3	-3	-3	-3	0	0	0	0	0	0	0	0	0	0	0	0	0

^a Relative error larger than 10% shown with a grey background.

Table 2. Relative error ΔR_{b0} ($N, r_b, r_c, r_p, \sigma, \beta$) in percent for $N = 2$ to 12, and $r_c = r_{c,min}$ (close spacing), $2r_b/3$ (moderate spacing), and $r_b - r_p$ (wide spacing) ^a. The pipe radius r_p is 0.0125 m.

r_b (mm)	σ	β	Close						Moderate						Wide					
			2	4	6	8	10	12	2	4	6	8	10	12	2	4	6	8	10	12
150	-0.33	0.25	3	7	7	7	7	7	0	1	2	3	5	6	1	3	6	9	14	19
		0.50	2	4	4	4	4	4	0	0	1	2	3	3	1	1	2	4	6	8
		1.00	0	0	0	0	0	0	0	0	0	0	0	0	0	0	0	0	0	0
		2.00	-2	-5	-6	-6	-7	-7	0	0	-1	-1	-2	-3	0	-1	-1	-2	-3	-3
	0.00	0.25	3	7	7	7	7	7	0	1	2	3	5	6	0	1	2	5	9	13
		0.50	2	4	4	4	4	4	0	0	1	2	3	3	0	0	1	2	4	6
		1.00	0	0	0	0	0	0	0	0	0	0	0	0	0	0	0	0	0	0
		2.00	-2	-5	-6	-6	-7	-7	0	0	-1	-1	-2	-3	0	0	-1	-1	-2	-3

Table 2. Cont.

r_b (mm)	σ	β	Close				Moderate				Wide									
			2	4	6	8	10	12	2	4	6	8	10	12						
0.33		0.25	3	7	7	7	7	7	0	1	2	3	5	6	0	0	1	2	5	10
		0.50	2	4	4	4	4	4	0	0	1	2	2	3	0	0	0	1	3	4
		1.00	0	0	0	0	0	0	0	0	0	0	0	0	0	0	0	0	0	0
		2.00	-2	-5	-6	-6	-7	-7	0	0	-1	-1	-2	-3	0	0	0	-1	-1	-2

^a Relative error larger than 10% shown with a grey background.

Table 3. Relative error ΔR_{b0} ($N, r_b, r_c, r_p, \sigma, \beta$) in percent for $N = 2$ to 12, and $r_c = r_{c,min}$ (close spacing), $2r_b/3$ (moderate spacing), and $r_b - r_p$ (wide spacing) ^a. The pipe radius r_p is 0.02 m.

r_b (mm)	σ	β	Close				Moderate				Wide									
			2	4	6	8	10	12	2	4	6	8	10	12						
	-0.33	0.25	3	6	6	6	6	6	0	1	1	2	3	4	1	3	4	7	9	13
		0.50	1	4	4	4	4	4	0	0	1	1	2	2	1	1	2	3	4	5
		1.00	0	0	0	0	0	0	0	0	0	0	0	0	0	0	0	0	0	0
		2.00	-2	-5	-5	-6	-6	-6	0	0	0	-1	-1	-2	0	-1	-1	-1	-2	-2
300	0.00	0.25	3	6	6	6	6	6	0	1	1	2	3	4	0	0	1	3	5	8
		0.50	1	4	4	4	4	4	0	0	1	1	2	2	0	0	1	1	2	4
		1.00	0	0	0	0	0	0	0	0	0	0	0	0	0	0	0	0	0	0
		2.00	-2	-5	-5	-6	-6	-6	0	0	0	-1	-1	-2	0	0	0	-1	-1	-2
	0.33	0.25	3	6	6	6	6	6	0	1	1	2	3	4	0	0	0	1	2	5
		0.50	1	4	4	4	4	4	0	0	1	1	2	2	0	0	0	0	1	2
		1.00	0	0	0	0	0	0	0	0	0	0	0	0	0	0	0	0	0	0
		2.00	-2	-5	-5	-6	-6	-6	0	0	0	-1	-1	-2	0	0	0	0	-1	-1

^a Relative error larger than 10% shown with a grey background.

9. Further Discussion and Concluding Summary

The newly developed zeroth-order multipole formula provides a fast, flexible, and accurate method for calculating the thermal resistance of energy piles. The newly presented zero-order multipole Formula (31) for R_{b0} may be used in virtually all engineering applications for energy piles with r_b greater than or equal to 0.3 m and r_p less than or equal to 0.02 m with pipes equally spaced on a circle. The relative error $\Delta R_{b0}(N, r_b, r_c, r_p, \sigma, \beta)$ may exceed 10% in a few odd cases, but the absolute error in such cases is very small. Furthermore, the zero-order multipole Formula (31) may also be used for all energy piles with r_b between 0.15 and 0.3 m and r_p less than or equal to 0.0125 m if N is less than or equal to 10, and β is greater than or equal to 0.25. For applications with r_p equal to 16 mm and r_b equal to 0.15 to 0.3 m, the zero-order multipole Formula (31) may be used if N is less than or equal to 8. The zero-order multipole formula may also be used for all energy pile applications if β is equal to 1 or N is equal to 2.

To the best of the authors' knowledge, zeroth-order multipole Formula (31) is the first, and the only closed-form formula published to date, that can be used to calculate the thermal resistance of energy piles with any number of heat exchanger pipes. The proposed formula marks a substantial improvement on the current practice of sizing energy piles with three or more U-pipes based on a guessed value of thermal resistance, which can lead to improperly sized systems. The explicit formula will facilitate designers to step beyond the limits of using a conservative thermal resistance estimate, and will enable them to optimize the energy pile design by making informed decisions about design choices, such as the position and the number of heat exchanger pipes in the pile. The proper sizing of energy piles will, in turn, allow for the overall system size to be reduced and the system performance to be improved.

A possible direction for future research is the development of higher-order multipole formulas for calculating the local thermal resistance of energy piles. The higher-order formulas will further improve the accuracy of the thermal resistance calculation, especially for small-diameter energy piles (less than 300 mm). The derivation of such formulas is expected in the near future and they will be presented soon in a sequel paper.

To conclude, in this paper, a closed-form Formula (31) for the thermal resistance of energy piles with any number of heat exchanger pipes evenly spaced on a concentric circle inside the pile periphery was derived. The proposed formula is based on the zero-order multipole approximation ($J = 0$) and considers only line heat sources at the pipes. It was demonstrated that the newly derived formula can calculate the thermal resistance of large-diameter energy piles ($r_b \geq 0.3$ m) with an accuracy better than 10% essentially under all conditions. The relative errors are less than or equal to 5% for over 99% of the 648 cases analyzed in this study. It was also demonstrated that the zero-order formula can also be used for smaller-diameter energy piles ($0.15 \leq r_b < 0.3$ m) for most conditions, except when the dimensionless pipe thermal resistance β is very small and the number N of heat exchanger pipes in the energy pile tops 8. For these specific cases and for energy piles with particularly smaller diameters ($r_b < 0.15$ m), the use of higher-order multipoles is recommended—closed-form formulas for which will be presented in our forthcoming papers. This paper also presents a handy Formula (35) for the minimum thermal resistance of energy piles when the pipes touch the periphery of the pile.

Author Contributions: Both authors contributed equally to the design, concept, and preparation of the manuscript. All authors have read and agreed to the published version of the manuscript.

Funding: This research received no external funding.

Conflicts of Interest: The authors declare no conflict of interest.

Nomenclature

h_p	Heat transfer coefficient between fluid and outer side of pipe wall, $W/(m^2 \cdot K)$, see Equation (19)
J	Number of multipoles, $J = 0, 1, 2 \dots$
N	Number of pipes in the energy pile; $N = 2$ for single U-tube
q_0	Heat rejection rate from each pipe to the ground, W/m
R_b	Local thermal resistance between fluid in the U-tube to the energy pile wall, $(m \cdot K)/W$
R_{b0}	Local thermal resistance for the zero-order, $(m \cdot K)/W$, see Equation (31)
R_{bmin}	Minimum local thermal resistance, $(m \cdot K)/W$, see Equation (38)
R_p	Total fluid-to-pipe resistance for a single pipe i.e., one leg of the U-tube, $(m \cdot K)/W$
r_b	Radius of the energy pile, m
r_c	Radius of the concentric circle, m, see Figure 2
r_p	Outer radius of heat exchanger pipe, m
T	Temperature, $^{\circ}C$
T_b	Energy pile wall temperature, $^{\circ}C$
T_{bav}	Average temperature at the energy pile wall, $^{\circ}C$
T_f	Mean fluid temperature inside the U-tube, $^{\circ}C$
β	Dimensionless thermal resistance of one U-tube leg, see Equation (2)
ΔR_{b0}	Relative error in local thermal resistance for zero-order, %
λ	Thermal conductivity of the ground, $W/(m \cdot K)$
λ_b	Thermal conductivity of the energy pile, $W/(m \cdot K)$
σ	Thermal conductivity ratio, dimensionless, see Equation (2)

Appendix A. Detailed Mathematical Derivations for the Temperature Field

Appendix A.1. Complex-Valued Line Heat Source

The complex-valued line heat source function $W_0(z, z_0)$ is the basic solution and a starting point for the multipole method:

$$W_0(z, z_0) = \begin{cases} \ln\left(\frac{r_b}{z-z_0}\right) + \sigma \cdot \ln\left(\frac{r_b^2}{r_b^2 - \bar{z} \cdot z_0}\right), & |z| \leq r_b, \\ (1 + \sigma) \cdot \ln\left(\frac{r_b}{z-z_0}\right) + \sigma \cdot \frac{1+\sigma}{1-\sigma} \cdot \ln\left(\frac{r_b}{z}\right), & |z| \geq r_b. \end{cases} \quad (A1)$$

The real part of the function $W_0(z, z_0)$ gives the temperature field for a line heat source at $z = z_0$ with the strength $q = 2\pi\lambda_b$ (W/m). It will satisfy the Laplace equation in pile and ground regions since it is the real part of an analytical function except for the right-hand top logarithm involving \bar{z} . However, this latter part is the complex-conjugate of the analytic logarithm function defined by (A3), and its real part will satisfy the Laplace equation. This is a bit tricky and must be kept in mind in the analyses and derivations below.

The following complex notations are used:

$$z = x + i \cdot y, \quad |z| = \sqrt{x^2 + y^2}, \quad \bar{z} = x - i \cdot y, \quad z_0 = x_0 + i \cdot y_0, \quad |z_0| < r_b - r_p. \quad (A2)$$

The complex-valued logarithm of any complex function $f(z)$ is defined by (7):

$$\ln(f(z)) = \ln(|f(z)|) + i \cdot \arg(f(z)), \quad -\pi < \arg(f(z)) \leq \pi \quad (A3)$$

The upper expression of (A1) is valid in the circular energy pile region and the lower one in the ground outside the pile. The first top logarithm represents an ordinary line heat source, while the second term represents a line source at the “mirror” point $z = r_b^2/\bar{z}_0$. The expressions in the two regions are constructed so that the real part, and the ensuing radial heat flux at the pile and ground sides, become equal at the pile radius $|z| = r_b$. This means that the real solution satisfies the two internal boundary conditions at the pile wall. The *average* temperature from the real part of $W_0(z, z_0)$ (which will determine T_{bav}) taken around the pile periphery is zero.

The real part of $W_0(z, z_0)$ will be used in the temperature fields below. The complex conjugate of z times z_0 may be replaced by z times the complex conjugate of z_0 :

$$\operatorname{Re}\left[\ln\left(\frac{r_b^2}{r_b^2 - \bar{z} \cdot z_0}\right)\right] = \ln\left(\frac{r_b^2}{|r_b^2 - \bar{z} \cdot z_0|}\right) = \ln\left(\frac{r_b^2}{|r_b^2 - z \cdot \bar{z}_0|}\right) = \operatorname{Re}\left[\ln\left(\frac{r_b^2}{r_b^2 - z \cdot \bar{z}_0}\right)\right]. \quad (A4)$$

The expression (A1) outside the pile (lower line) may be written in the following alternative way:

$$|z| \geq r_b : W_0(z, z_0) = \frac{1 + \sigma}{1 - \sigma} \cdot \ln\left(\frac{r_b}{z}\right) + (1 + \sigma) \cdot \ln\left(\frac{z}{z - z_0}\right), \quad \frac{1 + \sigma}{1 - \sigma} = \frac{\lambda_b}{\lambda}, \quad 1 + \sigma = \frac{2 \lambda_b}{\lambda_b + \lambda}. \quad (A5)$$

The first part presents a simple line source at the center $z = 0$ with the radial logarithmic temperature decrease $\ln(r_b/r)$. The second part tends to zero as $r = |z|$ increases and it determines the φ -dependence for $r > r_b$.

Appendix A.2. Temperature Field from N Line Heat Sources on a Circle

The (steady-state, real-valued) temperature field $T_c(z)$ for the pipes on the circle is to be determined for the prescribed heat flux q_0 (W/m) from all pipes, and any prescribed average temperature T_{bav} around the pile periphery. From this, the required fluid temperature T_f is to be determined from the boundary condition at the pipes. The thermal resistance R_b of the energy pile is then determined in accordance with (5).

The temperature field consists of a linear combination of the real part of the line heat source solution taken at the center of each pipe:

$$T_c(z) = T_{bav} + \frac{q_0}{2 \pi \lambda_b} \cdot \text{Re}[W_c(z, r_c)], \quad z_n = r_c \cdot z_e^n. \quad (A6)$$

$$W_c(z, r_c) = \begin{cases} \sum_{n=1}^N \left[\ln\left(\frac{r_b}{z - z_n}\right) + \sigma \cdot \ln\left(\frac{r_b^2}{r_b^2 - z \cdot \bar{z}_n}\right) \right], & |z| \leq r_b, \\ \frac{\lambda_b}{\lambda} \cdot \left[N \cdot \ln\left(\frac{r_b}{z}\right) + \frac{2 \lambda}{\lambda_b + \lambda} \cdot \sum_{n=1}^N \ln\left(\frac{z}{z - z_n}\right) \right], & |z| \geq r_b, \end{cases} \quad \bar{z}_n = r_c \cdot z_e^{-n}. \quad (A7)$$

where $W_c(z, r_c)$ is the sum of the N complex-valued line sources (A1) for the energy pile and ground regions. The “conjugate” substitution (A4) is used. The prescribed average temperature is to be added since the average temperature at the pile periphery is zero for each term in the sum. The factor before the sum ensures that the heat flux from each pipe is q_0 . The total heat flux from all pipes to the surrounding ground is $N \cdot q_0$ (W/m).

Equation (A6) is the line-source solution without using multipoles. The above temperature field satisfies the five conditions listed in Section 3.1 (after Equation (12)).

Appendix A.3. New Formulas for the Temperature Field

The sums in (A7) for $W_c(z, r_c)$ of the N complex-valued line sources involve two sums of logarithms:

$$\Sigma_1 = \sum_{n=1}^N \ln\left(\frac{r_b}{z - z_n}\right), \quad \Sigma_2 = \sum_{n=1}^N \ln\left(\frac{r_b^2}{r_b^2 - z \cdot \bar{z}_n}\right), \quad \bar{z}_n = r_c \cdot z_e^{-n}. \quad (A8)$$

The first sum of logarithms may be rewritten as a logarithm of products:

$$\Sigma_1 = \ln\left[\frac{r_b^N}{(z - r_c \cdot z_e^1) \cdot (z - r_c \cdot z_e^2) \cdot \dots \cdot (z - r_c \cdot z_e^N)} \right] = \ln\left(\frac{r_b^N}{z^N - r_c^N}\right). \quad (A9)$$

The roots of the polynomial $z^N - r_c^N = 0$ are $z = z_n, n = 1, \dots, N$. The two polynomials in the denominator of order N have the same roots. Hence, they are identical. The other sum of logarithms may, in the same way, be rewritten as:

$$\Sigma_2 = \ln\left[\frac{r_b^{2N}}{(r_b^2 - z \cdot r_c \cdot z_e^{-1}) \cdot \dots \cdot (r_b^2 - z \cdot r_c \cdot z_e^{-N})} \right] = \ln\left(\frac{r_b^{2N}}{r_b^{2N} - z^N \cdot r_c^N}\right). \quad (A10)$$

where, again, the two polynomials in the right-hand denominator of the logarithms are identical since they have the same roots:

$$r_b^{2N} - (z \cdot r_c)^N = 0 \Rightarrow z \cdot r_c \cdot z_e^{-n} = r_b^2, \quad n = 1, 2, \dots, N. \quad (A11)$$

It may be noted that the two left-hand expressions involving logarithms in (A9) and (A10) may differ by $2\pi i$ times an integer depending on the choice of arguments in the logarithms. However, this does not influence the real part used for the temperature field. This comment is applicable to the addition of logarithms in all other cases in this paper.

The complex-valued temperature field (A7) may now be written in the following concise form inserting the sums (A8)–(A10):

$$W_c(z, r_c) = \begin{cases} \ln\left(\frac{r_b^N}{z^N - r_c^N}\right) + \sigma \cdot \ln\left(\frac{r_b^{2N}}{r_b^{2N} - z^N \cdot r_c^N}\right), & |z| \leq r_b \\ \frac{\lambda_b}{\lambda} \cdot \left[N \cdot \ln\left(\frac{r_b}{z}\right) + \frac{2 \lambda}{\lambda_b + \lambda} \cdot \ln\left(\frac{z^N}{z^N - r_c^N}\right) \right], & |z| \geq r_b \end{cases}. \quad (A12)$$

These formulas are the starting point in Section 3.1, Equation (9). The above temperature fields depend on z^N . Let the point z be “rotated” m times by z_e .

$$(z_e^m \cdot z)^N = \left(e^{\frac{2\pi i}{N} \cdot m}\right)^N \cdot z^N = \left(e^{\frac{2\pi i}{N} \cdot N}\right)^m \cdot z^N = z^N \Rightarrow \operatorname{Re}[W_c(z_e^m \cdot z, r_c)] = \operatorname{Re}[W_c(z, r_c)]. \quad (\text{A13})$$

The real part of the temperature field repeats itself for any rotation $(z_e)^m$. This means that the temperature field is the same in every wedge with the opening angle $\Delta\varphi = 2\pi/N$ as indicated in Figure 2, left. The temperature field is also symmetric in y . It is sufficient to consider the temperature field in the wedge $0 \leq \varphi \leq \pi/N$, $r \geq 0$.

Figure 3 (left) and (right), in Section 5.2 show the temperature field from (A6) and (A12) for the reference case (39). The black circle $r = r_b = 0.3$ shows the periphery of the energy pile. The positions of the N pipes and the rotational symmetry ($N = 8$) are clearly seen.

References

1. Rees, S. (Ed.) *Advances in Ground-Source Heat Pump Systems*; Woodhead Publishing: Cambridge, UK, 2016.
2. Garber, D.; Choudhary, R.; Soga, K. Risk Based Lifetime Costs Assessment of a Ground Source Heat Pump (GSHP) System Design: Methodology and Case Study. *Build. Environ.* **2013**, *60*, 66–80. [\[CrossRef\]](#)
3. Rivoire, M.; Casasso, A.; Piga, B.; Sethi, R. Assessment of Energetic, Economic and Environmental Performance of Ground-Coupled Heat Pumps. *Energies* **2018**, *11*, 1941. [\[CrossRef\]](#)
4. Vieira, A.; Alberdi-Pagola, M.; Christodoulides, P.; Javed, S.; Loveridge, F.; Nguyen, F.; Cecinato, F.; Maranha, J.; Florides, G.; Prodan, I.; et al. Characterisation of Ground Thermal and Thermo-Mechanical Behaviour for Shallow Geothermal Energy Applications. *Energies* **2017**, *10*, 2044. [\[CrossRef\]](#)
5. Loveridge, F.; Powrie, W. Temperature response functions (G-functions) for single pile heat exchangers. *Energy* **2013**, *57*, 554–564. [\[CrossRef\]](#)
6. Loveridge, F.; Powrie, W.; Nicholson, D. Comparison of two different models for pile thermal response test interpretation. *Acta Geotech.* **2014**, *9*, 367–384. [\[CrossRef\]](#)
7. Park, H.; Lee, S.R.; Yoon, S.; Choi, J.C. Evaluation of thermal response and performance of PHC energy pile: Field experiments and numerical simulation. *Appl. Energy* **2013**, *103*, 12–24. [\[CrossRef\]](#)
8. Lamarche, L.; Kajl, S.; Beauchamp, B. A review of methods to evaluate borehole thermal resistances in geothermal heat-pump systems. *Geothermics* **2010**, *39*, 187–200. [\[CrossRef\]](#)
9. Javed, S.; Spittler, J.D. Calculation of borehole thermal resistance. In *Advances in Ground-Source Heat Pump Systems*, 1st ed.; Rees, S.J., Ed.; Woodhead Publishing: Cambridge, UK, 2016; pp. 63–95.
10. Javed, S.; Spittler, J.D. Accuracy of borehole thermal resistance calculation methods for grouted single U-tube ground heat exchangers. *Appl. Energy* **2017**, *187*, 790–806. [\[CrossRef\]](#)
11. Loveridge, F.; Powrie, W. 2D thermal resistance of pile heat exchangers. *Geothermics* **2014**, *50*, 122–135. [\[CrossRef\]](#)
12. Paul, N.D. The Effect of Grout Thermal Conductivity on Vertical Geothermal Heat Exchanger Design and Performance. Master’s Thesis, South Dakota University, Brookings, SD, USA, July 1996.
13. Sharqawy, M.H.; Mokheimer, E.M.; Badr, H.M. Effective pipe-to-borehole thermal resistance for vertical ground heat exchangers. *Geothermics* **2009**, *38*, 271–277. [\[CrossRef\]](#)
14. Bauer, D.; Heidemann, W.; Müller-Steinhagen, H.; Diersch, H.J. Thermal resistance and capacity models for borehole heat exchangers. *Int. J. Energy Res.* **2011**, *35*, 312–320. [\[CrossRef\]](#)
15. Diao, N.R.; Zeng, H.Y.; Fang, Z.H. Improvement in modeling of heat transfer in vertical ground heat exchangers. *HVAC R Res.* **2004**, *10*, 459–470. [\[CrossRef\]](#)
16. Bennet, J.; Claesson, J.; Hellström, G. *Multipole Method to Compute the Conductive Heat Flows to and between Pipes in a Composite Cylinder*; Notes on Heat Transfer 3; University of Lund: Lund, Sweden, 1987.
17. *Earth Energy Designer (EED)*, Version 4.2; BLOCON: Lund, Sweden, 2019.
18. *Ground Loop Heat Exchanger Professional (GLHEPro)*, Version 5.0; International Ground Source Heat Pump Association (IGSHPA): Stillwater, OK, USA, 2016.
19. Claesson, J.; Hellström, G. Multipole method to calculate borehole thermal resistances in a borehole heat exchanger. *HVAC R Res.* **2011**, *17*, 895–911.
20. Claesson, J.; Javed, S. Explicit multipole formulas for calculating thermal resistance of single U-tube ground heat exchangers. *Energies* **2018**, *11*, 214. [\[CrossRef\]](#)

21. Claesson, J.; Javed, S. Explicit multipole formulas and thermal network models for calculating thermal resistances of double U-pipe borehole heat exchangers. *Sci. Technol. Built Environ.* **2019**, *25*, 980–992. [[CrossRef](#)]
22. Nehari, Z. *Introduction to Complex Analysis*; Allen and Bacon Inc.: Boston, MA, USA, 1961.

Publisher’s Note: MDPI stays neutral with regard to jurisdictional claims in published maps and institutional affiliations.



© 2020 by the authors. Licensee MDPI, Basel, Switzerland. This article is an open access article distributed under the terms and conditions of the Creative Commons Attribution (CC BY) license (<http://creativecommons.org/licenses/by/4.0/>).